Nucleotide-Resolution Mapping of Topoisomerase-Mediated and Apoptotic DNA Strand Scissions at or near an *MLL* Translocation Hotspot

Marc-Edouard Mirault, Patrick Boucher, and Alain Tremblay

The emergence of therapy-related acute myeloid leukemia (t-AML) has been associated with DNA topoisomerase II (TOP2)–targeted drug treatments and chromosomal translocations frequently involving the *MLL,* or *ALL-1,* gene. Two distinct mechanisms have been implicated as potential triggers of t-AML translocations: TOP2-mediated DNA cleavage and apoptotic higher-order chromatin fragmentation. Assessment of the role of TOP2 in this process has been hampered by a lack of techniques allowing in vivo mapping of TOP2-mediated DNA cleavage at nucleotide resolution in single-copy genes. A novel method, extension ligation-mediated polymerase chain reaction (ELMPCR), was used here for mapping topoisomerase-mediated DNA strand breaks and apoptotic DNA cleavage across a translocation-prone region of *MLL* in human cells. We report the first genomic map integrating translocation breakpoints and topoisomerase I, TOP2, and apoptotic DNA cleavage sites at nucleotide resolution across an *MLL* region harboring a t-AML translocation hotspot. This hotspot is flanked by a TOP2 cleavage site and is localized at one extremity of a minor apoptotic cleavage region, where multiple single- and double-strand breaks were induced by caspase-activated apoptotic nucleases. This cleavage pattern was in sharp contrast to that observed ~200 bp downstream in the exon 12 region, which displayed much stronger apoptotic cleavage but where no double-strand breaks were detected and no t-AML–associated breakpoints were reported. The localization and remarkable clustering of the t-AML breakpoints cannot be explained simply by the DNA cleavage patterns but might result from potential interactions between TOP2 poisoning, apoptotic DNA cleavage, and DNA repair attempts at specific sites of higher-order chromatin structure in apoptosis-evading cells. ELMPCR provides a new tool for investigating the role of DNA topoisomerases in fundamental genetic processes and translocations associated with cancer treatments involving topoisomerase-targeted drugs.

The stabilization of DNA topoisomerase II (TOP2) cleavage complexes by specific poisons converts this enzyme into a potent genotoxin.[1,2] Studies of DNA cleavage induced in vivo by TOP2-targeted drugs, such as epipodophyllotoxins (e.g., etoposide and teniposide) and anthracyclines (e.g., doxorubicin and epirubicin), are clinically very relevant because these drugs are widely used to treat leukemias, lymphomas, and various cancers, including breast and ovarian cancers, but are increasingly suspected to be at the origin of secondary cancers (reviewed by Pedersen-Bjergaard and Rowley,[3] Felix,[4] and Pui and Relling[5]). A case in point is the emergence of therapy-related acute myeloid leukemia (t-AML), which is frequently associated with the use of TOP2-targeted drugs and can occur in up to 10% of children who receive treatment for acute lymphoblastic leukemia. These drugs are strongly suspected to induce recurrent chromosomal translocations at specific loci, some of which may persist in surviving cells and confer a selective growth advantage to leukemogenic cells. Recurrent translocations observed in 33% of 511 therapy-related acute leukemia or myelodysplastic syndrome cases involved the myeloid-lymphoid (or mixed lineage) leukemia gene (*MLL,* or *ALL-1* [MIM 159555]) on chromosome 11 band q23[6] and in-frame fusion with 1 of >40 partner genes (reviewed by Rowley[7]). Virtually all *MLL* translocation breakpoints are clustered in a particular region of the gene called the "breakpoint cluster region." *MLL* is a human homolog of the *Drosophila* gene *trithorax,* a positive regulator of gene expression during development. It encodes a histone H3 lysine 4–specific methyltransferase, which regulates target *Hox* gene expression.[8] It is not required for initiation of gene activity but maintains transcriptional states through later stages of development. Recombinant disruption of *MLL* may generate fusion proteins leading to leukemic transformation,[9] which strongly suggests that deregulation of *Hox* gene expression is critical for *MLL*-associated leukemogenesis.

Despite the strong epidemiological link supporting a causative involvement of TOP2 in induction of t-AML–associated translocations, the direct implication of TOP2 in this process has remained elusive. Although several studies have tentatively localized drug-induced TOP2 cleavage sites at or close to translocation breakpoints,[4,10,11] their identification was based on homology to published TOP2 "consensus sequences" or on in vitro cleavage of cloned DNA by TOP2. The assumption that the in vitro cleavage sites reflect genuine TOP2 cleavage sites in vivo (in chromatin) has been challenged,[12–14] and bona fide lo-

From the Department of Medicine, Université Laval, and Unit of Health and Environment, Centre de Recherche du Centre Hospitalier Universitaire de Québec–Centre Hospitalier de l'Université Laval, Quebec City

Received May 3, 2006; accepted for publication July 18, 2006; electronically published September 12, 2006.

Address for correspondence and reprints: Dr. Marc-Edouard Mirault, Unité de Santé et Environnement, Local 9700, Centre de Recherche du CHUL, 2705 Boulevard Laurier, Quebec City, Quebec, Canada G1V 4G2. E-Mail: memirault@crchul.ulaval.ca

Am. J. Hum. Genet. 2006;79:779–791. 0002-9297/2006/7905-0002$15.00

calization of in vivo TOP2 cleavage sites in the vicinity of *MLL* translocation breakpoints, at nucleotide resolution, has not yet been reported. On the other hand, higher-order chromatin fragmentation occurring during drug-induced apoptosis was proposed as an alternative mechanism for initiation of t-AML–associated chromosomal translocations.[15] In support of this, in vitro experiments with cultured cells revealed that activation of apoptotic effector nucleases alone was sufficient to generate proleukemogenic translocations and suggested that some of these may persist in cells that evade apoptosis and divide.[16] Thus, it is not clear whether TOP2-mediated DNA strand breaks or DNA cleavage produced by subsequently activated apoptotic nucleases is at the origin of the recurrent chromosomal translocations observed in t-AML.

Although conventional ligation-mediated PCR (LMPCR) is a powerful tool for genomic sequencing, in vivo footprinting of protein-DNA complexes, and mapping of various forms of DNA damage at genomic sites of interest (reviewed by Pfeifer and Riggs[17] and Drouin et al.[18]), the scope of DNA-damage detection by LMPCR is intrinsically limited to DNA lesions, which produce, directly or indirectly, DNA strand breaks with 5′-phosphate (5′-P) termini required for linker ligation. This limitation excludes the use of LMPCR for detection of several DNA lesions, including those mediated by type II and type IA DNA topoisomerases, which generate transient DNA strand breaks with enzyme-linked 5′ termini (reviewed by Liu[1] and Wang[2]). The difficulty in mapping in vivo TOP2-mediated DNA cleavage at nucleotide resolution in single-copy genes is highlighted by the absence of related publications, despite the development of versatile methods such as single-strand ligation PCR[19] and terminal transferase–dependent PCR,[20] which were primarily designed to detect covalent adduct formation by DNA-damaging agents.

In the present study, a different procedure, extension LMPCR (ELMPCR), was used for genomic mapping of DNA strand breaks that escape detection by conventional LMPCR because of formation of 5′ termini different from 5′-P. We show that a combination of ELMPCR and LMPCR is a powerful tool for genomic mapping of topoisomerase-mediated strand breaks and apoptotic DNA cleavage at single-nucleotide resolution in human cells. We report the first genomic map integrating translocation breakpoints and drug-induced DNA cleavages mediated by TOP2, topoisomerase I (TOP1), or caspase-activated DNases at nucleotide resolution across translocation-prone and apparently translocation-exempt regions of the *MLL* gene. Although a strong in vivo TOP2 cleavage site and a major apoptotic cleavage region were identified in *MLL* exon 12, both were localized >200 bp downstream of a remarkable cluster of t-AML–related translocation breakpoints located in intron 11. This translocation hotspot was flanked by another TOP2 cleavage site and was localized within a minor apoptotic cleavage region featuring multiple caspase-dependent double-strand breaks (DSBs) not observed in exon 12. Although the issue of the relationship of the translocation breakpoints to DNA cleavage by TOP2 or an apoptotic nuclease was not resolved, this study demonstrates that ELMPCR provides an efficient tool for high-resolution mapping of in vivo TOP2 DNA cleavage sites. This is of importance because cellular TOP2 cleavage sites were found to be different from those observed in vitro with purified enzyme or those predicted from putative "consensus" sequences.

Material and Methods

Cell Culture and Treatments

Primary human skin fibroblasts were grown in high-glucose/HEPES Dulbecco's modified Eagle's medium (Sigma) supplemented with sodium pyruvate (0.11 g/liter), antibiotic antimycotics, and 5% fetal bovine serum (FBS). Human Epstein-Barr virus (EBV)–transformed B-lymphoblastoid P6 cells, T-lymphoblastoid CEM cells (ATCC line CCRF-CEM), and TOP2α-mutant CEM/VM-1 cells deficient in TOP2 activity[21,22] were cultured in RPMI 1640 medium containing 10% FBS. Confluent cultures of fibroblasts or of growing P6 or CEM cells were incubated in the presence of etoposide (VP-16 [Novopharm], purchased as a physiologic solution for patient treatment and diluted in medium), camptothecin (CPT) (Sigma), or CD95 antibody (clone CH11 [Upstate]), which was added to the medium at concentrations indicated in the figures. After medium removal at the end of treatment, the cells were covered with or resuspended into 2 ml PBS and were incubated for 15 min at 60°C—to reverse TOP2- and TOP1-mediated DNA cleavage—or were not incubated, before DNA isolation. Of note, heat treatment at this temperature was sufficient to revert efficiently the topoisomerase-mediated DNA cleavages observed in cells, in contrast to reversion of in vitro TOP2α cleavage reactions, which are reported to require a higher temperature.[23] Alternatively, reversion was also performed by 30-min incubation of drug-treated cells at 37°C in the absence of drug and in complete medium.

DNA Isolation

Minimizing artefactual background DNA damage during DNA isolation is critical for maximizing (E)LMPCR detection of physiologically relevant DNA cleavage. Genomic DNA was extracted from *intact* cells, to avoid any possible enzymatic DNA cleavage associated with cell fractionation. The resuspended cells were lysed by addition of 2 ml of 2× lysis buffer and 11 ml of lysis buffer (50 mM Tris-HCl [pH 7.4], 20 mM EDTA [pH 7.4], 1% SDS, 10 μM deferoxamine mesylate (Sigma), and 0.5 mg/ml proteinase K) and were incubated overnight at 37°C. To remove proteinase K, protein salting-out was performed by addition of 2/5 volumes of saturated NaCl to 1 volume of cell lysate, followed by mixing and centrifugation for 15 min at 20,200 *g*; the DNA-containing supernatant was recentrifuged at 20,200 *g* and was precipitated with 2 volumes absolute ethanol (for 30 min at −70°C and 15 min at 1,100 *g* at 4°C). DNA pellets were rinsed once with 80% ethanol and were recentrifuged at 1,100 *g*. After complete removal of the ethanol, wet DNA pellets were dissolved in 200 μl autoclaved ultrapure water (PURELAB Ultra water purification system [Elga]). To remove RNA, each sample was incubated at 37°C for 1 h in 300 μl of 10-mM Tris-HCl (pH 8.0), 1-mM EDTA (pH 8.0),

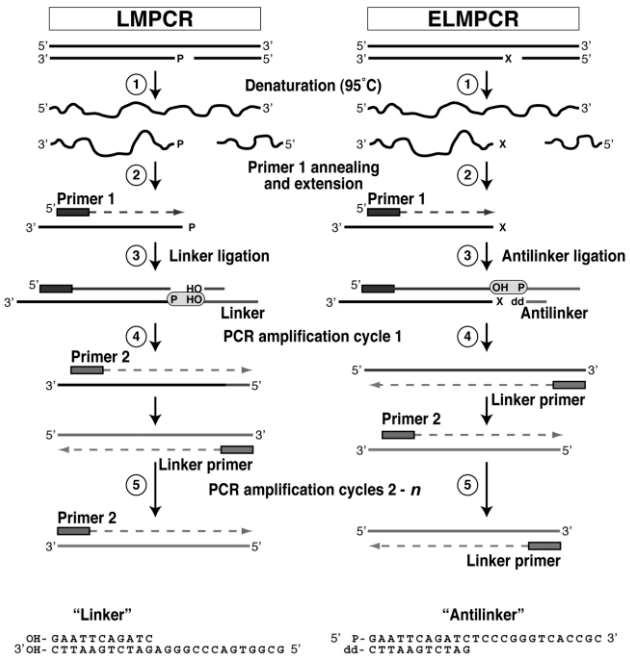

Figure 1. Distinctive features of ELMPCR compared with those of conventional LMPCR. LMPCR requires a 5′-phosphate (P) at the 5′ end of a genomic DNA break for linker ligation, in contrast to ELMPCR, which involves ligation of an antilinker (with a sequence complementary to the LMPCR linker) to the 3′-hydroxyl(OH) end of a primer 1 extension product.

and 0.17-mg/ml heat-treated DNase-free RNase A (Roche), followed by addition of 300 μl of 2× proteinase K buffer (200 mM NaCl, 50 mM EDTA [pH 8.0], 10 mM Tris-HCl [pH 8.0], 1% SDS, and 1 mg/ml proteinase K [Invitrogen]) and incubation at 37°C for 1 h and 50°C for 1 h. Proteinase K was removed by salting-out (as described above) followed by phenol extraction. The phenol quality is of critical importance for minimizing oxidative damage to the DNA during extraction. We used pH-8.0 buffer-equilibrated ultrapure phenol (MB grade [USB]) containing 0.1% 8-hydroxyquinoline (Sigma). The DNA was extracted with 1 volume of phenol-chloroform-isoamylalcohol (50:48:2), followed by one chloroform extraction and ethanol precipitation (2 volumes). After cooling at −70°C for 30 min and centrifugation at 9,300 *g* for 5 min, DNA pellets were washed once with 80% ethanol, were resuspended in 400 μl TE (10-mM Tris-HCl and 1-mM EDTA [pH 8.0]), and were reprecipitated overnight at −20°C with 2.5 volumes ethanol after addition of 40 μl of 5-M NaCl. After one wash with 80% ethanol, wet DNA pellets were dissolved in 200 μl of 1-mM Tris-HCl (pH 8.0) for 48–72 h at 4°C, including gentle mixing by hand several times a day. After complete DNA dissolution, residual traces of ethanol were eliminated by incubation at 65°C for 5 min (in open tubes). Note that DNA samples were never put on vortex and were always treated so as to minimize DNA shearing, and they were not desiccated, to avoid oxidation and to facilitate DNA dissolution in aqueous buffers. The DNA concentration (~0.5 μg/μl) was measured by diphenylamine assay and/or fluorometry by use of a TKO-100 DNA fluorometer in accordance with the instructions of the manufacturer (Hoefer Scientific Instruments).

LMPCR and ELMPCR

LMPCR was performed essentially by the method of Drouin et al.,[18] with the use of *Pfu* exo$^-$ polymerase in the primer extension step.[24] The distinctive feature of ELMPCR is that a 5′-phosphorylated asymmetric "antilinker" is ligated to the 3′-OH termini of the primer 1 extension products (fig. 1). The long and short antilinker oligonucleotides were 5′-P-GAATTCAGATCTCCCGGGTCACCGC-3′ and 5′-GATCTGAATTddC-3′ (Keystone Labs), respectively, with the latter carrying a (2′,3′)-dideoxy-cytidine (ddC) or a 3′-phosphate at the 3′ end, to prevent interlinker ligation. Similar ELMPCR results were obtained with these two modified 3′ ends (fig. 2). ELMPCR amplification was done as for LMPCR, except that the linker-primer concentration was doubled, to compensate for the loss of single-strand linker-primer resulting from annealing to residual complementary antilinker oligonucleotides. LMPCR and ELMPCR reactions were run in a PTC-100 or PTC-200 DNA engine (MJ Research). All primers (table 1) were selected using computer programs as described elsewhere.[18]

Optimization of buffer and temperature conditions for primer 1 extension.—Optimal conditions of *Pfu* exo$^-$-mediated primer 1 extension were determined by testing which of the 12 buffers of the Opti-Prime PCR Optimization Kit (Stratagene) or standard *Pfu* buffer containing 2 mM or 4 mM $MgSO_4$ gives the best yield of expected PCR product generated by a pair of primers 1, by use of 75 ng cellular DNA, 1.5 pmol of each sense and antisense primer 1 to be used together, 250 μM of each dNTP, and 0.75 U *Pfu* exo$^-$ in 15 μl optimal buffer (in 0.2-ml tubes) across 25 PCR cycles (at 95°C for 60 s, average primer 1 annealing temperature [T_m] for 60 s, and 74°C for 60 s) following an initial step at 95°C for 5 min. After incubation at 74°C for 10 min at the end, the PCR products were analyzed on agarose gels. The optimal temperature (T_{opt}) was determined by running 12 PCR reactions with the optimal buffer over a temperature gradient from the average primer 1 T_m − 4°C to the average primer 1 T_m + 11°C, by use of a PTC-200 equipped with a temperature gradient head (MJ Research).

Primer 1 annealing.—Cellular DNA (1.6 μg) was incubated with 1.25 pmol primer 1 in 25 μl optimal buffer for 20 min at primer 1 T_{opt} (table 1) after 3 min of incubation at 98°C.

Primer 1 extension.—Primer 1 extension was performed at T_{opt} by addition of 5 μl (containing 1.5 mM of each dNTP and 1.5 U *Pfu* exo$^-$) to the 25 μl of annealed DNA and incubation from T_{opt} to 74°C at 0.1°C temperature increase per second and for 10 min at 74°C, followed by a return to 4°C, a cooling on ice, and a quick spin. The asymmetric double-stranded linker and antilinker were freshly prepared by annealing of the 25-mer oligonucleotides to their respective complementary 11-mer oligonucleotides, as described by Drouin et al.[18]

Ligation.—Ligation reactions were performed by addition of a

The figure is available in its entirety in the online edition of *The American Journal of Human Genetics*.

Figure 2. Comparison of efficiency of antilinkers terminated by a 3′-phosphate-deoxycytidine or a 2′,3′-dideoxycytidine in ELMPCR detection of topoisomerase-mediated DNA cleavage. The legend is available in its entirety in the online edition of *The American Journal of Human Genetics*.

Table 1. Primers and Optimized Conditions Used for Primer Extension and PCR Amplification

The table is available in its entirety in the online edition of *The American Journal of Human Genetics*.

45-μl ligation cocktail (containing, for 10 reactions, 15 μl of 1-M dithiothreitol, 7.6 μl of 100-mM ATP, 7.6 μl of 1-M $MgCl_2$, 7.6 μl of 0.1-M spermidine, 9.2 μl BSA at 5 mg/ml, 16 μl of 2-M Tris-HCl [pH 7.4], 50 μl linker or 10 μl antilinker at 20 pmol/μl, 6.6 μl T4 DNA ligase [5 U/μl; Roche], and H_2O, to total 450 μl) to the 30-μl primer 1 extension mixtures and by incubation overnight at alternating temperature cycles: 10°C for 30 s and 22°C for 30 s. The ligation reactions were stopped on ice by addition of 30 μl containing 28 μl of 7.5-M NH_4OAc, 1 μl of 0.5-M EDTA, and 1 μl glycogen at 20 mg/ml and were transferred to 0.5-ml thick-wall tubes. The DNA was precipitated by addition of 275 μl ice-cold ethanol and centrifugation at 15,800 *g* for 20 min at 4°C (Microfuge). DNA pellets were rinsed once with 0.5 ml of 80% ethanol, were centrifuged at 15,800 *g* for 8 min, and were resuspended in 25 μl H_2O. The DNA solution was heated at 65°C for 10 min (in open tubes).

Optimization of primer 2–mediated PCR amplification.—Primers 2 used in this study are listed in table 1, with optimal buffer and temperature conditions determined as follows and with pairs of primer sets as indicated. Each optimal buffer was determined by testing which of 10 *Taq* buffers supplemented with 2, 4, 6, 8, or 10 mM $MgCl_2$ or with 2, 4, 6, 8, or 10 mM $MgCl_2$ plus 15 mM $(NH_4)_2SO_4$ gives the best yield of expected PCR product, by use of 1 μg cellular DNA, 10 pmol of each sense and antisense primer 2 to be used together, 200 μM of each dNTP, and 3 U *Taq* DNA polymerase in 100-μl PCR reactions (in 0.5-ml tubes) across 25 PCR cycles (at 95°C for 60 s, average primer 2 T_m for 60 s, and 74°C for 60 s) following an initial step at 95°C for 5 min. After 10 min at 74°C, the PCR products were analyzed on agarose gels. T_{opt} was determined as described above, by 12 PCR reactions run with the optimal buffer over a temperature gradient from average primer 2 T_m − 4°C to average primer 2 T_m + 11°C.

LMPCR and ELMPCR.—The amplification reactions were performed in 100 μl optimal *Taq* buffer (10 mM Tris-HCl [pH 8.9], 40 mM NaCl, and 0.01% gelatin, supplemented with $MgCl_2$ and $(NH_4)_2SO_4$ as indicated in table 1) containing 1.6 μg ligated DNA (25 μl; see above), 10 pmol primer 2, 10 pmol (for LMPCR) or 30 pmol (for ELMPCR) linker-primer, 200 μM of each dNTP, and 3 U *Taq* polymerase (Amersham Biosciences), overlaid with 50 μl mineral oil. PCR amplification was performed for 22 cycles (for LMPCR[18]) or 26 cycles (for ELMPCR), as follows: 1 cycle at 95°C for 300 s, T_{opt} for 180 s, and 74°C for 180 s; 1 cycle at 95°C for 60 s, T_{opt} − 1°C for 150 s, and 74°C for 180 s; 1 cycle at 95°C for 60 s, T_{opt} − 2°C for 120 s, and 74°C for 180 s; 1 cycle at 95°C for 60 s, T_{opt} − 3°C for 120 s, and 74°C for 180 s; 1 cycle at 95°C for 60 s, T_{opt} − 4°C for 90 s, and 74°C for 150 s; 13 (for LMPCR) or 17 (for ELMPCR) cycles at 95°C for 60 s, T_{opt} − 4°C for 90 s + 5 s per cycle, and 74°C for 150 s + 5 s per cycle; 1 cycle at 95°C for 60 s, T_{opt} − 3°C for 240 s, and 74°C for 240 s; 1 cycle at 95°C for 60 s, T_{opt} − 2°C for 240 s, and 74°C for 240 s; 1 cycle at 95°C for 60 s, T_{opt} − 1°C for 240 s, and 74°C for 240 s; 1 cycle at 95°C for 60 s, T_{opt} for 240 s, and 74°C for 600 s; followed by a 4°C hold. Each reaction (100 μl) was stopped by addition of 25 μl of 2.5-M NaCl and 60-mM EDTA (pH 8.0), followed by one phenol-chloroform extraction (250 μl of 30:50), DNA precipitation with 2.5 volumes ethanol, centrifugation, and washing with 80% ethanol, as described above. Air-dried DNA pellets were resuspended in 10 μl of sequencing gel loading buffer and were heated at 65°C for 15 min. The DNA samples were heated at 95°C for 2 min just before analysis by gel electrophoresis (60-cm-long, 8% polyacrylamide-TBE [0.09-mM Tris-borate {10.8 g/liter Tris and 5.5 g/liter boric acid} and 0.0025 EDTA {pH 8.0}] sequencing gels), electroblotting to nylon membranes, and hybridization to ^{32}P-radiolabeled single-strand probes, by use of the same equipment and methodology described by Drouin et al.[18] After hybridization, the membranes were washed once in 2 × SSPE and 0.1% SDS at room temperature for 15 min and once in 1 × SSPE and 0.1% SDS at 55°C for 15 min. After air drying, the membranes were exposed in a PhosphorImager (Storm 860 [GE Healthcare]), and the signals were analyzed with ImageQuant TL software (v2003.01 [Amersham Biosciences/GE Healthcare]).

DNA cleavage mapping.—Nucleotide-resolution mapping of DNA strand scissions was achieved by in-gel alignment of (E)LMPCR signals with Maxam and Gilbert DNA sequencing ladders after optimal reduction or magnification of signal intensity and blowup of the gel region to be analyzed, to maximize band resolution. Cleavage mapping was performed by at least two investigators and was confirmed in at least three independent analyses involving each duplicate ELMPCR reaction, and, in several cases, different primer sets.

Most potential problems and recommendations regarding genomic sequencing by conventional LMPCR[17,18] hold for ELMPCR. Careful selection of primers (e.g., absence of repetitive DNA and a melting temperature match) and optimization of PCR conditions with the selected primers (see above) are of paramount importance to maximize (E)LMPCR success rate. ELMPCR usually requires three more PCR amplification cycles than does LMPCR to yield comparable signal intensities at 5′-P DNA cleavage sites (e.g., restriction enzyme–mediated cleavages). This difference was primarily due to the fivefold lower antilinker concentration in ELMPCR compared with the linker concentration in LMPCR and possibly also to the different blunt-end structures of the two linkers. In addition, it is not known whether there are potentially negative effects of 5′-end–linked adducts on ligation efficiency. The relative ELMPCR signal intensities measured at an in vivo TOP2 cleavage site by use of serial twofold dilutions of cellular DNA were linearly related to cleaved DNA concentration (R^2 = 0.997) (fig. 3), which showed that ELMPCR signal intensities can be used to evaluate relative extents of DNA cleavage at specific sites.

Results

ELMPCR

In contrast to conventional LMPCR, which requires genomic 5′-P DNA termini for linker ligation, ELMPCR was designed so that linker ligation does not depend on the

The figure is available in its entirety in the online edition of *The American Journal of Human Genetics*.

Figure 3. Linear relationship between ELMPCR signal intensity and the extent of TOP2-mediated DNA cleavage. The legend is available in its entirety in the online edition of *The American Journal of Human Genetics*.

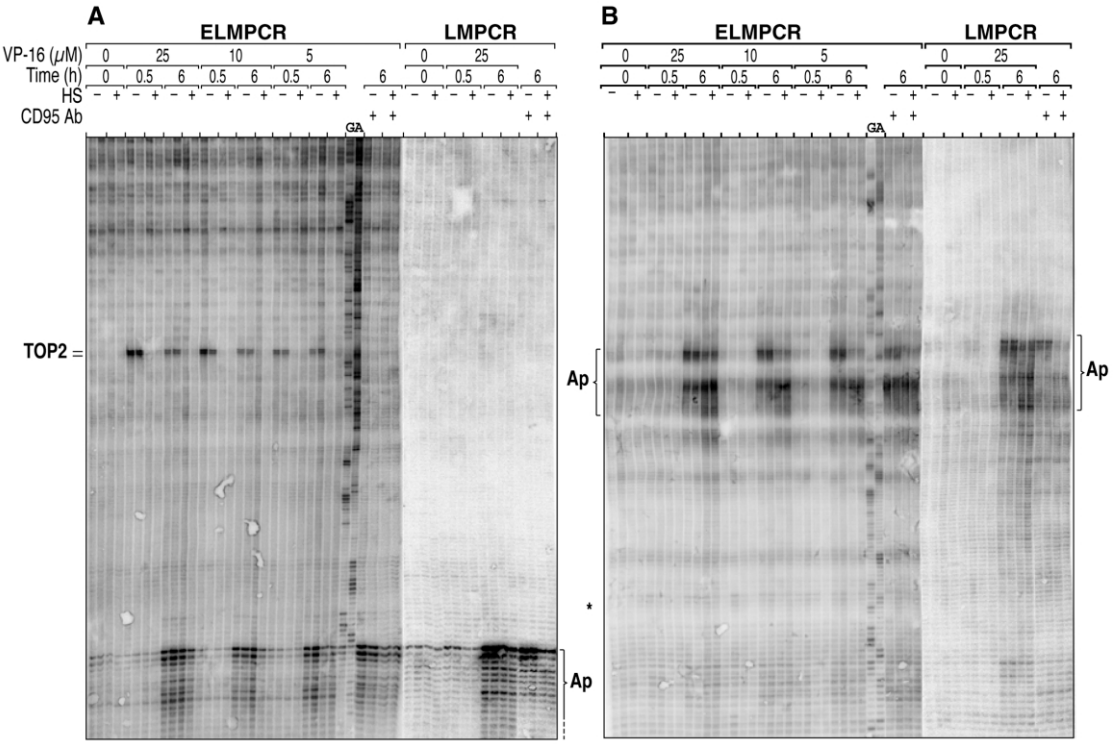

Figure 4. Distinction of apoptotic versus TOP2-mediated DNA cleavage by combined use of ELMPCR and LMPCR. Human P6 lymphoblastoid cells were treated or were not treated (controls) with VP-16 or with CD95 antibody (Ab) to induce apoptosis. Part of the cells was then heat shocked (HS) at 60°C for 15 min to reverse topoisomerase-mediated DNA cleavage before DNA extraction. ELMPCR and LMPCR data are from duplicate cell cultures, by use of set 1 primers for noncoding-strand analysis (*A*) and set 2 primers for the coding-strand analysis (*B*). The TOP2 cleavage site is at 6909/6910, and the apoptotic cleavage region (Ap) extends upstream of 6816 on the noncoding strand (*A*) and downstream of 6816 on the coding strand (*B*) (see fig. 9). The asterisk (*) in panel B indicates the expected position for a reciprocal TOP2 cleavage, which was not detected, opposite to the TOP2 cleavage site identified on the coding strand. TOP2 cleavage positions indicate 5′ nucleotides covalently linked to the enzyme. Lanes G and A are Maxam and Gilbert DNA sequencing ladders. The ELMPCR and LMPCR exposure intensities were normalized to DNA sequencing ladders.

5′-end structures generated at DNA breaks. As shown below, ELMPCR permits genomic mapping of topoisomerase-mediated DNA strand breaks featuring enzyme-linked 5′ ends, such as those produced by type II and type IA DNA topoisomerases. Because the topoisomerase tyrosine residues (or oligopeptides) bound to the 5′-P termini cannot be removed by proteinase K treatments used to extract the DNA (see the "Material and Methods" section), these blocked 5′-phosphates cannot be ligated to linkers and thus cannot be detected by conventional LMPCR. The distinctive features of ELMPCR are illustrated in figure 1. The central difference between ELMPCR and other LMPCR methods is that ELMPCR targets direct ligation of an antilinker to the 3′-hydroxyl terminus of a primer-extended DNA molecule, instead of ligation of a conventional linker to a 5′-P terminus of genomic DNA (in LMPCR) or linker ligation to linearly amplified primer-extended single-strand DNA[19] or terminal transferase–elongated DNA.[20] The antilinker nucleotide sequence is complementary to that of the LMPCR linker, so that the same linker primer can be used in both LMPCR and ELMPCR protocols. Note also that the short antilinker oligonucleotide carries a (2′,3′)-dideoxy cytidine at the 3′ end, to prevent inter-antilinker ligation. Except for these intrinsic differences, all PCR amplification and subsequent steps are similar in both procedures. The capacity of ELMPCR to detect TOP2-mediated DNA cleavage and LMPCR-detectable strand breaks had been validated using restriction enzyme–cleaved DNA and in vitro TOP2 DNA cleavage reactions (M. L. Fournier, personal communication, and A.T. and M.-E.M., unpublished data). Because the same linker primer can be used in LMPCR and ELMPCR, the combination of both techniques provides a unique way to directly distinguish, in the same sequencing gel, DNA strand breaks yielding 5′-P from those producing non–5′-P termini, as demonstrated below.

Analysis of Topoisomerase-Mediated and Apoptotic DNA Strand Cleavage across MLL *Exon 12–Intron 12 Region*

A combination of ELMPCR and LMPCR was used for genomic mapping of TOP2-mediated and apoptotic DNA

The figure is available in its entirety in the online edition of *The American Journal of Human Genetics*.

Figure 5. Colocalization of etoposide- and teniposide-induced TOP2 DNA cleavage. The legend is available in its entirety in the online edition of *The American Journal of Human Genetics*.

cleavage in the exon 12–intron 12 area, a genomic region apparently exempt of t-AML–related chromosomal translocations. EBV-immortalized B-lymphocytes (P6 cells) were treated with etoposide for a short time (30 min) so that etoposide-induced TOP2-mediated DNA cleavage could be detected in the absence of significant apoptotic DNA cleavage. Longer treatments (6 h) were also administered, to assess apoptotic DNA cleavage, which follows initial etoposide-mediated stabilization of TOP2-DNA cleavage complexes. In contrast to fully viable untreated cells, these treatments induced apoptosis and complete loss of cell viability, as checked by flow cytometry analysis performed as described elsewhere.[26] Combined use of the two LMPCR procedures permitted distinction of DNA strand breaks mediated by TOP2 (enzyme-linked 5′ ends) from those resulting from apoptosis-related nucleolytic cleavage that produces 5′-P termini. Representative ELMPCR cleavage patterns are presented in figure 4*A*, which shows a major doublet TOP2 cleavage detected after 30 min of exposure to clinically relevant etoposide concentrations.[27] This cleavage signal persisted after 6 h of exposure, although at reduced intensity. Detection of this cleavage was highly reproducible in multiple experiments using different sets of primers and different cell types, including human fibroblasts and lymphoblastoid CEM cells (see below), as well as T47D breast carcinoma cells (not shown). Several lines of evidence indicate that this cleavage was mediated by TOP2: (1) it was rapidly and dose-dependently induced by etoposide (fig. 4*A*) and was produced at the same position in response to teniposide, another specific and widely used TOP2 poison (fig. 5); (2) cleavage was reversible by heat shock, a characteristic feature of drug-stabilized TOP2 cleavage complexes[1]; and (3) etoposide-induced strand cleavage at this site was strongly reduced in a TOP2α-mutant CEM/VM-1 cell line deficient in TOP2 activity[21,22] compared with in parental CEM cells (see below). TOP2-mediated strand breaks were not detected by LMPCR (fig. 4*A*, right), as expected. In contrast, clustered redundant strand breaks that were most evident after 6 h of etoposide treatment were efficiently detected by both LMPCR and ELMPCR. The similar pattern of strand breaks induced by Fas receptor (CD95) antibody (fig. 4*A*), a classic inducer of apoptosis acting via receptor activation and not DNA damage, and their suppression by preincubation of the cells with the pan-caspase inhibitor zVAD-fmk (see below) indicate that they were mediated by caspase-activated nucleases, apparently involved in both Fas and DNA-damage apoptotic pathways. In contrast, TOP2-mediated cleavage was not affected by zVAD-fmk. Figure 4*B* shows the corresponding ELMPCR and LMPCR cleavage patterns detected with a set of primers targeting the opposite (coding) strand of the exon 12 region. No TOP2-mediated cleavage was detected on this strand after 30 min of exposure to etoposide (fig. 4*B*), administered at concentrations up to 100 μM (not shown). Reciprocal TOP2 cleavage opposite to the TOP2 cleavage site identified on the noncoding strand (fig. 4*A*) was not detected. However, strong DNA cleavage clustered in two adjacent hotspots was detected by both ELMPCR and LMPCR after 6 h of drug exposure, which validated the ELMPCR capacity to detect strand breaks with this set of primers. This multiple cleavage was apoptosis related and caspase dependent, since it was induced by anti-CD95 antibody (fig. 4*B*) and was completely suppressed by zVAD-fmk (fig. 6). Although the ELMPCR and LMPCR patterns were very similar, minor differences were observed in relative signal intensities in the upper part of the respective apoptotic cleavage patterns, which are thought to reflect a statistical effect of the larger number of DNA strand breaks detected by ELMPCR. Of note, heat treatment of the cells to revert TOP2-mediated DNA cleavage caused a visible shift of the upper (E)LMPCR bands toward smaller products, probably reflecting heat-mediated enhancement of an endogenous DNA degradation process associated with apoptosis.

Human primary fibroblasts and T-lymphoblastoid CEM cells treated with etoposide produced DNA cleavage patterns very similar to those obtained using P6 cells (figs. 7 and 8 and data not shown). These cells were also exposed to CPT, a TOP1 poison, which stabilizes single-strand breaks (SSBs) in TOP1 cleavage complexes yielding enzyme-linked 3′ ends and 5′-hydroxyl termini.[2] Showing that ELMPCR can be used for genomic mapping of TOP1 cleavage sites was relevant because it has been suggested that TOP1-mediated DNA cleavage might contribute to apoptotic DNA cleavage.[28,29] CPT-induced TOP1-mediated strand scissions, not directly detectable by LMPCR, were thus mapped by ELMPCR in the *MLL* translocation-prone region and served as positive controls for strand-break detection, in case TOP2-mediated cleavage was not detected. Figure 7 shows the ELMPCR results obtained using primary human fibroblasts treated with etoposide or CPT for 1 h. Etoposide produced a major heat-reversible TOP2-mediated DNA cleavage at a unique doublet site on the noncoding strand (fig. 7*A*), identical to that found in P6

The figure is available in its entirety in the online edition of *The American Journal of Human Genetics*.

Figure 6. Caspase-dependent nucleolytic cleavage, distinguished from TOP1-mediated DNA cleavage. The legend is available in its entirety in the online edition of *The American Journal of Human Genetics*.

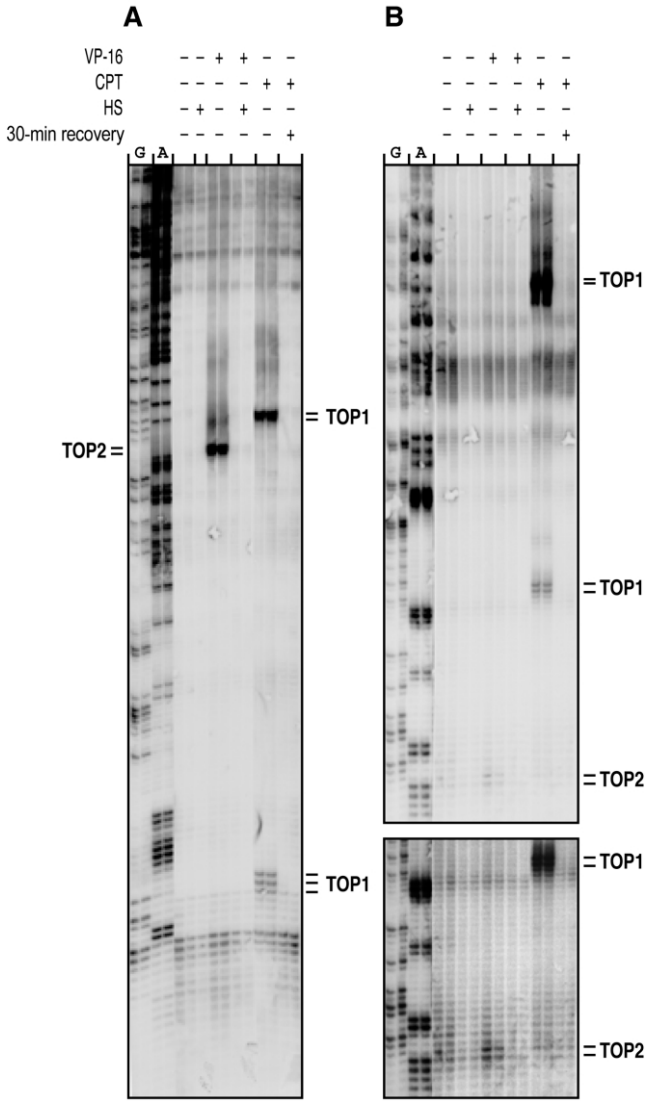

Figure 7. ELMPCR detection of TOP1- and TOP2-mediated DNA cleavage in primary human fibroblasts. Confluent fibroblast cultures were treated or were not treated (controls) with VP-16 (50 μM) or CPT (10 μM) for 1 h. Part of the cells was then heat shocked (HS), to reverse topoisomerase-mediated DNA cleavage. ELMPCR data were from duplicate cell cultures, by use of set 1 primers for the noncoding strand (*A*) and set 2 primers for the coding strand (*B*). A stronger exposure of the bottom part of panel B is shown below it, to enlarge the signal of a weak TOP2-mediated cleavage. Cleavage sites are at 6909/6910 for TOP2 and 6822/6823/6824 and 6920/6921 for TOP1 on the noncoding strand and at 6891/6892 and 6811/6812 for TOP1 on the coding strand (see fig. 9 map). TOP2 and TOP1 cleavage positions indicate the nucleotides covalently linked to the enzyme (5′-linked TOP2 and 3′-linked TOP1). Lanes G and A are Maxam and Gilbert DNA sequencing ladders.

cells (fig. 4*A*). No reciprocal cleavage was detected on the opposite (coding) strand, as in P6 cells. However, a heat-reversible TOP2 cleavage was detected 11–12 bp downstream of the expected reciprocal cleavage site (fig. 7*B*). ELMPCR revealed several CPT-induced SSBs, which could be reversed by 30-min cell recovery in the absence of drug (fig. 7*A* and 7*B*) or by heat shock (not shown). In addition, an unrelated cleavage ladder of weak signal intensity was observed in fibroblasts growing in the absence of drug, visible at the bottom of figure 7*A* and in the middle of figure 7*B*. Similar cleavage was enhanced by apoptosis in P6 cells (fig. 4*A* and 4*B*) and was unexpectedly strong in confluent healthy fibroblast cultures (A.T. and M.-E.M., unpublished data).

As shown in figure 8*A* and 8*B*, reciprocal double-strand DNA cleavage produced by the restriction enzyme *Apo*I was used as a positive control in the search for reciprocal TOP2-mediated DNA cleavage opposite to the major TOP2 site 6909/6910 in response to etoposide poisoning. An *Apo*I cleavage site was located 12 nt upstream of the doublet TOP2 cleavage site. This endonuclease generates 3′-recessed 4-base staggered double-strand cuts similar to reciprocal cleavage by TOP2. ELMPCR performed with a 0.6% dilution of *Apo*I-cleaved CEM DNA (extensive cleavage to completion) yielded cleavage signals of intensity comparable to that of the signals produced in vivo by TOP2 (fig. 8*A*). Similar ELMPCR results were obtained with *Pfu* exo$^-$- or Sequenase-mediated (GE Healthcare Life Sciences) primer extension, confirming that no etoposide-induced cleavage could be detected on the other strand at the position expected for a reciprocal TOP2 cleavage opposite to site 6909/6910, in contrast to positive detection of reciprocal *Apo*I cleavage with *Pfu* exo$^-$- or Sequenase-mediated primer extension, or Sequenase-filled 3′-recessed termini instead of primer extension (fig. 8*B*). The unexpected shorter *Apo*I cleavage products seen in figure 8*A* and 8*B* apparently reflect some contaminating nucleolytic activity present in the commercial *Apo*I preparation, since they did not occur in partial *Apo*I cleavage reactions (A.T., unpublished data).

Supportive evidence that the DNA cleavage detected at site 6909/6910 was mediated by TOP2 is provided by the ELMPCR results presented in figure 8*C*. Teniposide-resistant CEM/VM-1 cells, which are deficient in TOP2α activity[21] because of a single base substitution–altering enzyme interaction with ATP,[22] showed strongly reduced DNA cleavage at site 6909/6910 in response to etoposide, compared with parental CEM cells expressing wild-type TOP2α. Cleavage at this site was thus predominantly mediated by TOP2α in CEM cells, whereas that observed in VM-1 cells probably resulted from normal TOP2β and/or residual TOP2α activity. In contrast, a similar extent of heat-reversible DNA cleavage was observed in VM-1 and CEM cells at a nearby TOP2 site located on the opposite strand (6917/6918) in response to 100-μM etoposide treatments for 60 min. The latter observation leads us to speculate that cleavage at this second TOP2 site was predom-

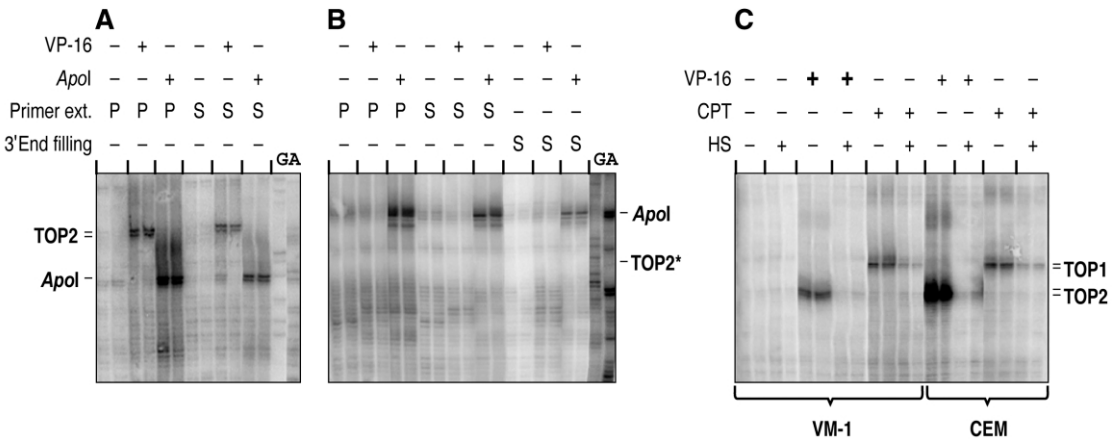

Figure 8. TOP2-mediated DNA cleavage in CEM and TOP2α-mutant CEM/VM-1 cells. Cells were treated with 25 μM or 100 μM (indicated by larger plus sign [+]) VP-16 or 5 μM CPT for 30 min. ELMPCR was performed with equal amounts of DNA isolated from duplicate drug-treated cell cultures or from untreated cultures including 0.6% CEM DNA cleaved to completion by restriction endonuclease *Apo*I. *A* and *B,* ELMPCR with primer extension (ext.) performed with *Pfu* exo$^-$ (P) or Sequenase (S) or PCR amplification after Sequenase-mediated filling of 3′-recessed termini (with no heat denaturation and no primer 1 extension) and antilinker ligation (*B*), by use of set 1 primers (*A*) or set 10 primers (*B*). In panel C, set 1 primers were used. The noncoding-strand cleavage sites for TOP2, TOP1, and *Apo*I are 6909/6910, 6920/6921, and 6897, respectively. No reciprocal TOP2 cleavage was detected on the coding strand (TOP2* at 6906/6907).

inantly mediated by TOP2β, which is not affected in VM-1 cells.

Colocalization of Topoisomerase-Mediated and Apoptotic DNA Strand Cuts at a Major MLL *Translocation Hotspot*

DNA cleavage analysis was then focused on the intronic region upstream of *MLL* exon 12, where therapy-related leukemia translocation breakpoints are unusually clustered across a very short region (~10 bp)[11,30,31] (fig. 9). Figure 10 displays ELMPCR data covering a region including the translocation hotspot and the exon 12 apoptotic cleavage region. A striking finding is the quasi colocalization of TOP1, TOP2, and apoptotic cleavage sites within the translocation hotspot, at the upstream extremity of the intronic apoptotic cleavage region (fig. 9). After 30 min of etoposide exposure, a heat-reversible TOP2 (doublet) cleavage was reproducibly detected on the coding strand at position 6583/6584, a few nucleotides upstream of a major CPT-TOP1 cleavage site located within the translocation hotspot (fig. 10*B*). No TOP2-mediated DNA cleavage was detected on the opposite strand. Three reversible CPT-TOP1 cleavage sites were identified on the noncoding strand, all located in apoptotic cleavage regions (fig. 10*A*). Remarkably similar apoptotic cleavage patterns were produced in cells incubated for 6 h with CD95 antibody, etoposide, or CPT. All strand scissions induced in the apoptotic cleavage regions were apparently mediated by caspase-activated nucleases, since they were completely suppressed by zVAD-fmk (fig. 6).

DSBs are dangerous DNA lesions that can cause cell death or promote illegitimate DNA recombination events in surviving cells. The possible production of DSBs in the upstream apoptotic cleavage region was assessed by LMPCR amplification by use of cellular DNA from etoposide-treated cells (6 h of treatment) directly ligated to LMPCR linker or ELMPCR antilinker (without primer extension). The data shown in figure 10*C* demonstrate the occurrence of multiple blunt DSBs and potential staggered DSBs, several of which were localized within or close to the translocation hotspot (fig. 9). In sharp contrast, similar formation of multiple DSBs was not observed in the major downstream apoptotic cleavage region (exon 12), where no therapy-related translocation breakpoints have been reported.

Discussion

We describe here a novel LMPCR procedure, ELMPCR, which allows direct mapping of in vivo topoisomerase-mediated DNA strand breaks in single-copy genes at nucleotide resolution. We present the first nucleotide-resolution map integrating in vivo TOP2- and TOP1-mediated strand breaks and apoptotic DNA cleavages in a human gene segment, illustrating the potential of this method. This high-resolution map across both translocation-prone and translocation-exempt regions of *MLL* reveals several findings of interest with regard to the nature of the respective DNA cleavages and their position relative to known translocation breakpoints.

All but one of the TOP2-mediated strand breaks were localized relatively far from the translocation hotspot, with the dominant TOP2 cleavage site located >300 bp

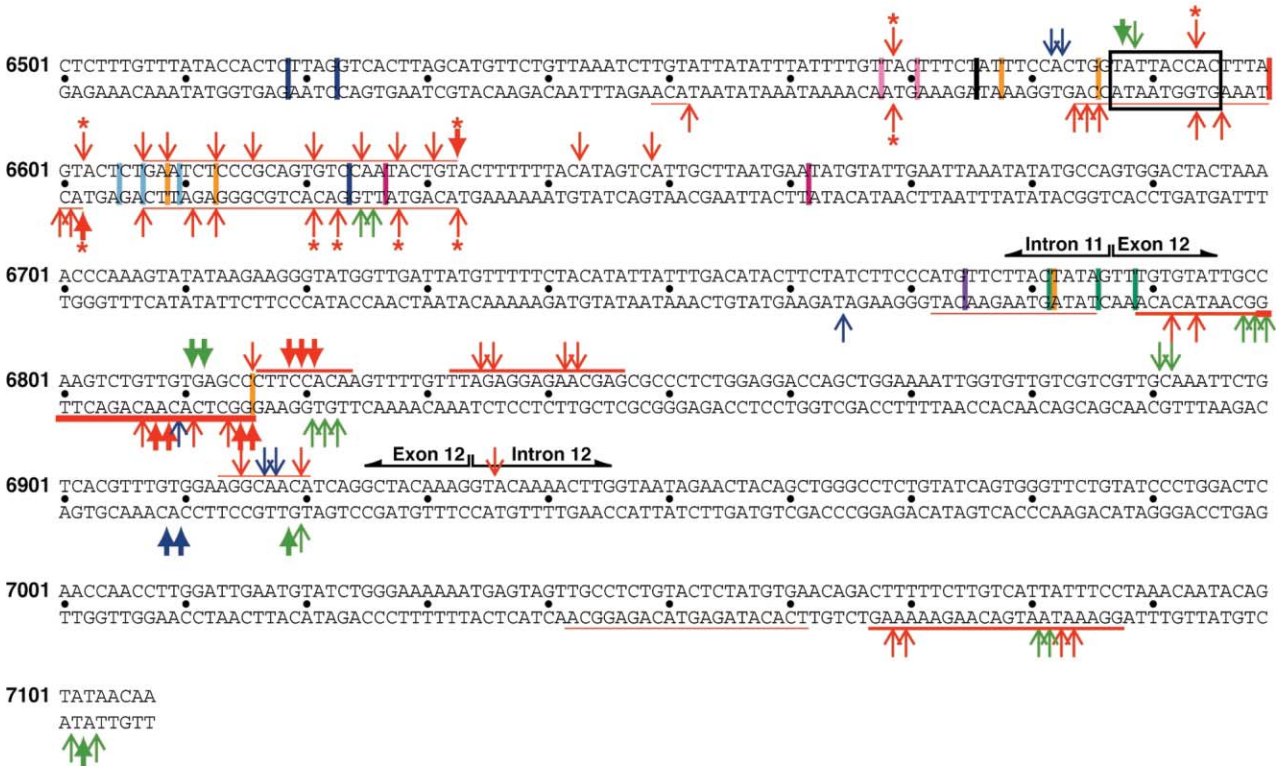

Figure 9. Nucleotide-resolution map of topoisomerase DNA cleavage sites, apoptotic cleavage hotspots, and translocation breakpoints. The map integrates the results of multiple ELMPCR and LMPCR analyses performed as described in figures 4, 7, 8, and 10, by use of all sets of primers listed in table 1. The coding strand is the upper strand. *Blue arrows,* Etoposide-induced TOP2 cleavage sites. *Green arrows,* CPT-induced TOP1 cleavage sites. Hotspots for apoptotic cleavage are shown underlined in red (thick line indicates stronger cleavage). *Red arrows,* Predominant cleavage sites (thick arrows indicate stronger cleavage sites). Asterisks (*) indicate blunt DSBs. The black box defines a major translocation hotspot, which includes nine therapy-related translocation breakpoints associated with multidrug treatments involving TOP2-targeted drugs,[11,30,31,32] and the breakpoint reported for a cell line (SN-1) derived from a patient with T-cell acute lymphoblastic leukemia with no history of previous treatment.[32] Vertical marks show additional translocation breakpoints reported in the literature,[30,31,33,34] with each color corresponding to a different patient, except for all orange breakpoints, which resulted from Fas-mediated apoptosis in vitro.[35,16] Duplicate marks of same color reflect uncertainties about the exact *MLL* breakpoint location because of local overlapping of DNA sequences at the *MLL*-partner junction or because of sequence gaps between derivative *MLL* and derivative partner breakpoints.

downstream, in exon 12 (or exon 9 according to an older numbering system). This observation does not support a potential involvement of these sites as *direct* triggers of *MLL* translocations. To our knowledge, no translocation breakpoints have been reported near the dominant TOP2 cleavage sites mapped in exon 12. Of interest, these TOP2 cleavage sites were located in a translocation-exempt region covering most of exon 12 and downstream intron 12 sequences. In contrast, one TOP2 cleavage site detected at the border of the t-AML translocation hotspot might be at the origin of the *MLL/AF-9* translocation breakpoint junction reported by Whitmarsh et al.[11] The very close proximity of this TOP2 site to multiple apoptotic DNA cleavages observed at and near the translocation hotspot is consistent with potential interactions between TOP2 and caspase-activated DNase(s)[36] and with a possible role of TOP2 as translocation initiator at this site.[11] ELMPCR mapping of in vivo TOP2 cleavage sites and apoptotic DNA scissions in *AF-9* and other known *MLL* fusions, including novel partner genes identified by long-distance inverse PCR,[37] should help assess the respective role of TOP2 and apoptotic DNA fragmentation in t-AML–associated leukemogenic translocations.

Of interest, none of the in vivo TOP2 cleavage sites identified here were found to correspond to in vitro–determined consensus TOP2 cleavage sequences reported in exon 12 (6857–6874[38,39]). Thus, the best-fit matches to putative consensus sequences are poor predictors of bona fide cellular TOP2 cleavage sites. Moreover, no DNA cleavage was observed at these cellular TOP2 cleavage sites in reactions performed in vitro with human TOP2α and DNA isolated from CEM cells or PCR-amplified *MLL* DNA (A.T. and M.-E.M., unpublished data). These observations strongly suggest that local chromatin structure and DNA accessibility are the primary determinants of TOP2 cleavage site specificity in vivo, as proposed elsewhere.[13,14] If

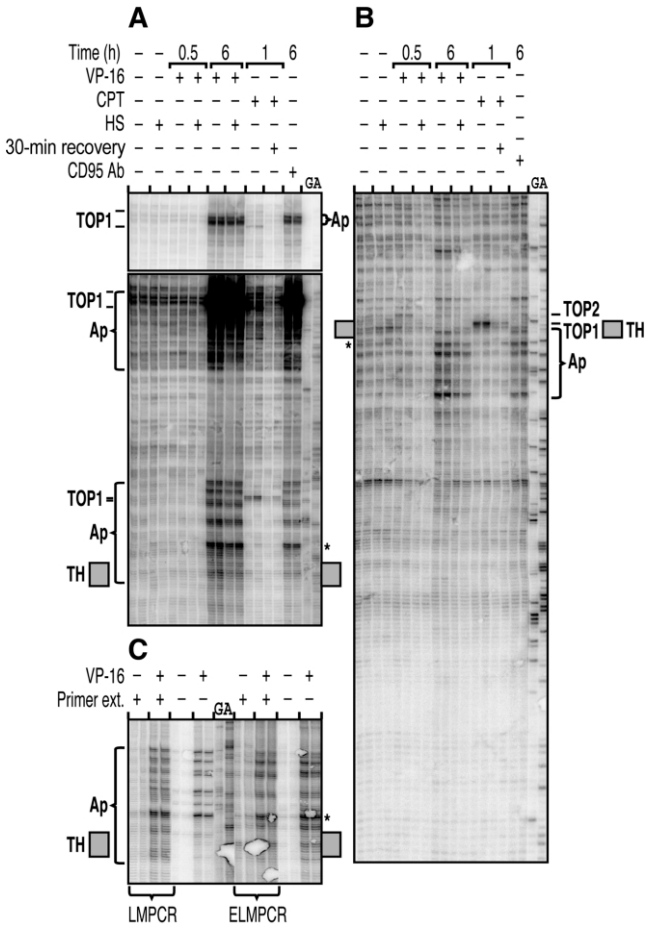

Figure 10. Colocalization of apoptotic and topoisomerase-mediated DNA cleavages at a major *MLL* translocation hotspot. CEM cells were treated with etoposide (100 μM), CPT (5 μM), or CD95 antibody (Ab) for the time indicated. ELMPCR data were from duplicate cell cultures, by use of set 7 primers for noncoding-strand cleavage analysis (*A*) and set 4 primers for coding-strand analysis (*B*). The upper panel in A shows a lower exposure of the top portion of the main panel. Cleavage sites are 6822/23, 6801, and 6626/27 for TOP1 on the noncoding strand (*A*) and 6588/89 for TOP1 and 6583/84 for TOP2 on the coding strand (*B*). *C,* Detection of blunt DSBs by direct PCR amplification after linker or antilinker ligation (no heat denaturation and no primer 1 extension), as compared with LMPCR (*left*) or ELMPCR (*right*), respectively. The apoptotic cleavage regions (Ap) extend from 6816–6773 (*top*) and 6633–6585 (*bottom*) on the noncoding strand (*A*), and from 6633–6595 on the coding strand (*B*); an asterisk (*) indicate cleavages forming a major blunt DSB at 6602/6603. The TH side boxes locate the translocation hotspot (fig. 9). Lanes G and A are Maxam and Gilbert DNA sequencing ladders. HS = heat shocked.

so, local in vivo TOP2 cleavage site specificity and frequency might differ in different cell types, depending on the differentiation state and associated chromatin structure at the investigated site. Although the dominant in vivo TOP2 cleavage sites observed in this study were located at identical positions in several unrelated cell types, it is possible that the chromatin context of the *MLL* intron 11–exon 12 region in these cells may differ from that prevailing in the leukemogenic precursor cells in which the t-AML translocations occur, whose identity is usually unknown. It will thus be important to identify these leukemogenic precursor cells for future studies of the relationships between localized chromatin structure, apoptotic and TOP2-mediated DNA cleavage, and translocation breakpoints.

The observation that etoposide treatments produced predominantly TOP2-mediated SSBs in the *MLL* region analyzed, regardless of the cell type investigated, is of interest, considering that normal TOP2 function (no inhibitor) involves transient cleavage of *both* DNA strands.[1,2] Our ELMPCR results are consistent with those of previous studies reporting predominant formation of SSBs in cultured cells exposed to etoposide[1,40] and in TOP2 cleavage reactions performed in vitro at low drug concentrations.[41] The single-strand scissions detected here may reflect the asymmetric action of an individual etoposide molecule stabilizing one strand-specific nick, with little drug effect on TOP2 cleavage/religation of the opposite DNA strand scission.[41,42] With regard to recombination potential, one should keep in mind that TOP2-mediated SSBs may be converted to DSBs by collisions with replication forks or transcription complexes, similar to trapped TOP1 cleavage complexes.[2,43,44]

The strongest apoptotic DNA cleavage across the *MLL* gene region investigated occurred in exon 12, in all cell types investigated. This major apoptotic cleavage region would include the *MLL* site-specific cleavage reported elsewhere[15,38] and the colocalized in vivo TOP2 cleavage and DNase I hypersensitive sites mapped at lower resolution by Southern analysis[45,46] (exon 9 in those studies corresponds to exon 12 in the present study[47]). The apoptotic cleavage pattern observed here at nucleotide resolution in exon 12 is peculiar and quite distinct from that produced in the upstream intronic region containing the translocation hotspot (fig. 9). The exon 12 cleavage pattern might reflect an initial endonucleolytic cleavage followed by 5′→3′ exonucleolytic processing of each strand. This apparent double-strand cleavage site is located at the dyad symmetry center of an inverted repeat, 5′-TTGTGN$_8$CACAA, a structure that might provide potential binding sites for DNA cleaving enzyme(s), including TOP1, found to cleave both 5′-TTGTG motifs (on opposite strands) in response to CPT poisoning. A future challenge will be to determine which apoptotic nucleases may cause the observed zVAD-fmk–sensitive DNA degradation process. Of interest, the unique potential double-strand cleavage site detected in this apoptotic cleavage region was found to precisely correspond to one *MLL* translocation breakpoint at site 6816 observed in cultured cells engaged in Fas receptor–mediated apoptosis.[16] Three additional Fas-induced translocation breakpoints[35] were also localized within apoptotic DNA cleavage regions (fig. 9), supporting the view that repair of an initial (or partial) ap-

optotic DNA cleavage by nonhomologous end joining[33] may produce chromosomal translocations in viable cells escaping irreversible apoptotic execution.[15,16,35,48] The occurrence of multiple nicks, potential staggered DSBs, and blunt cuts detected in the minor apoptotic cleavage region harboring the t-AML breakpoint cluster suggests that such DNA lesions, undergoing variable extents of DNA repair,[32,33,35] are likely to be at the origin of these translocations. Intronic illegitimate recombination of *MLL* with one of many potential gene partners, after DNA cleavage and attempted repair, would favor formation of in-frame fusion leukemogenic oncogenes.[7,9,32,49] Expression of oncogenes conferring tumor-cell growth advantage is likely to play a major role in selecting breakpoints that lie within an intron rather than within an exon. Although apoptotic DNA cleavage, per se, apparently can be a sufficient condition to produce *MLL/AF9* translocations in cultured cells,[16] another mechanism is required to explain why t-AML balanced translocations are preferentially associated with chemotherapeutic treatments involving TOP2-targeted drugs[3,4,6] but not with any cytotoxic agent. It thus will be important to determine whether TOP2-mediated DNA cleavage can induce illegitimate recombination events at translocation hotspots in *MLL* and relevant target gene partners in the absence of apoptotic DNA cleavage. Second, it will be important to determine whether TOP2 poisoning or catalytic inhibition may indirectly stimulate DSB formation at such sites in surviving cells. For example, initial apoptotic cleavage of higher-order chromatin loops by a caspase-activated DNase might be triggered by alteration(s) of DNA/chromatin structure or chromatin remodeling resulting from TOP2 dysfunction.

The striking association of CPT and TOP1 cleavage sites with apoptotic DNA cleavage regions is intriguing. It may be related to the suggestion that TOP1-mediated DNA cleavage can contribute to chromatinolysis in apoptosis.[29,50] Although most SSBs induced by CPT in the present study did not correspond to apoptotic DNA cleavage sites mapped in this *MLL* region, it remains possible that some of the zVAD-fmk–sensitive DNA cleavages observed in etoposide-treated cells could have been mediated by TOP1 after recruitment or activation consequent to single-strand DNA cleavage induced by caspase-activated nucleases.[51]

ELMPCR is, to our knowledge, the first PCR-based technique used successfully to map in vivo TOP2-mediated DNA cleavage in single-copy genes at single-nucleotide resolution. Previous analyses of drug-induced TOP2 cleavage sites in living cells were based on genomic primer-extension techniques and were restricted to satellite DNA repeats and multicopy genes, because of their intrinsically limited detection capacity.[14,52] In principle, ELMPCR should be suitable to map any topoisomerase-mediated strand break, including TOP3-mediated DNA cleavage and meiosis-specific DSBs catalyzed by TOP2-like Spo11 family proteins, which also involve enzyme-linked 5′ ends.[2,53] In addition, ELMPCR provides a potential new tool for mapping other types of DNA lesions producing, directly or indirectly, strand breaks with non–5′-P termini.

The observation of ELMPCR cleavage doublets at several cellular TOP2 and TOP1 cleavage sites is intriguing because DNA strand scissions produced in vitro by TOP2 or various restriction enzymes were essentially detected as single-nucleotide cleavage positions by ELMPCR (M. Fournier, personal communication, and A.T. and M.-E.M., unpublished data), thus ruling out a trivial artifact intrinsic to the technique. Further work will be required to clarify the origin of the apparent TOP2 cleavage degeneracy observed in this and other studies[52] and to determine whether this phenomenon reflects some topoisomerase flexibility with regard to in vivo cleavage site specificity.

In summary, the work reported here validates the experimental potential of ELMPCR for genomic mapping of topoisomerase-mediated DNA cleavage. The nature and relative distribution of the observed cleavages with regard to t-AML translocation breakpoints suggest that several DNA cleaving mechanisms, including topoisomerase poisoning and apoptotic nuclease(s), may interact to produce DSBs at sites prone to recombination events. The localization and remarkable clustering of some t-AML breakpoints cannot be simply explained by the observed DNA cleavage patterns but might result from potential interactions between TOP2 poisoning, apoptotic DNA cleavage, and DNA repair attempts at specific sites of higher-order chromatin structure.

Acknowledgments

We thank Ronald Hancock, Masahiko S. Sato, Girish Shah, and Michèle L. Fournier, for critically reading the manuscript, and William T. Beck, Edward W. Khandjian, and Régen Drouin, for providing, respectively, the cell lines VM-1/CEM and P6 and primary human fibroblasts. This work was supported by operating grant 012290 from the National Cancer Institute of Canada, with funds from the Canadian Cancer Society.

Web Resources

The accession number and URLs for data presented herein are as follows:

GenBank, http://www.ncbi.nlm.nih.gov/Genbank/ (for *MLL* sequence [accession number U04737])
Online Mendelian Inheritance in Man (OMIM), http://www.ncbi.nlm.nih.gov/Omim/ (for *MLL/ALL-1*)

References

1. Liu LF (1989) DNA topoisomerase poisons as antitumor drugs. Annu Rev Biochem 58:351–375
2. Wang JC (1996) DNA topoisomerases. Annu Rev Biochem 65: 635–692
3. Pedersen-Bjergaard J, Rowley JD (1994) The balanced and the unbalanced chromosome aberrations of acute myeloid leukemia may develop in different ways and may contribute differently to malignant transformation. Blood 83:2780–2786
4. Felix CA (1998) Secondary leukemias induced by topoisomerase-targeted drugs. Biochim Biophys Acta 1400:233–255

5. Pui CH, Relling MV (2000) Topoisomerase II inhibitor-related acute myeloid leukaemia. Br J Haematol 109:13–23
6. Rowley JD, Olney HJ (2002) International workshop on the relationship of prior therapy to balanced chromosome aberrations in therapy-related myelodysplastic syndromes and acute leukemia: overview report. Genes Chromosomes Cancer 33:331–345
7. Rowley JD (1998) The critical role of chromosome translocations in human leukemias. Annu Rev Genet 32:495–519
8. Milne TA, Briggs SD, Brock HW, Martin ME, Gibbs D, Allis CD, Hess JL (2002) MLL targets SET domain methyltransferase activity to *Hox* gene promoters. Mol Cell 10:1107–1117
9. Corral J, Lavenir I, Impey H, Warren AJ, Forster A, Larson TA, Bell S, McKenzie AN, King G, Rabbitts TH (1996) An *Mll-AF9* fusion gene made by homologous recombination causes acute leukemia in chimeric mice: a method to create fusion oncogenes. Cell 85:853–861
10. Lovett BD, Lo Nigro L, Rappaport EF, Blair IA, Osheroff N, Zheng N, Megonigal MD, Williams WR, Nowell PC, Felix CA (2001) Near-precise interchromosomal recombination and functional DNA topoisomerase II cleavage sites at *MLL* and *AF-4* genomic breakpoints in treatment-related acute lymphoblastic leukemia with t(4;11) translocation. Proc Natl Acad Sci USA 98:9802–9807
11. Whitmarsh RJ, Saginario C, Zhuo Y, Hilgenfeld E, Rappaport EF, Megonigal MD, Carroll M, Liu M, Osheroff N, Cheung NK, Slater DJ, Ried T, Knutsen T, Blair IA, Felix CA (2003) Reciprocal DNA topoisomerase II cleavage events at 5′-TATTA-3′ sequences in *MLL* and *AF-9* create homologous single-stranded overhangs that anneal to form der(11) and der(9) genomic breakpoint junctions in treatment-related AML without further processing. Oncogene 22:8448–8459
12. Capranico G, Jaxel C, Roberge M, Kohn KW, Pommier Y (1990) Nucleosome positioning as a critical determinant for the DNA cleavage sites of mammalian DNA topoisomerase II in reconstituted simian virus 40 chromatin. Nucleic Acids Res 18:4553–4559
13. Udvardy A, Schedl P (1991) Chromatin structure, not DNA sequence specificity, is the primary determinant of topoisomerase II sites of action in vivo. Mol Cell Biol 11:4973–4984
14. Kas E, Laemmli UK (1992) *In vivo* topoisomerase II cleavage of the *Drosophila* histone and satellite III repeats: DNA sequence and structural characteristics. EMBO J 11:705–716
15. Stanulla M, Wang J, Chervinsky DS, Thandla S, Aplan PD (1997) DNA cleavage within the *MLL* breakpoint cluster region is a specific event which occurs as part of higher-order chromatin fragmentation during the initial stages of apoptosis. Mol Cell Biol 17:4070–4079
16. Betti CJ, Villalobos MJ, Diaz MO, Vaughan AT (2003) Apoptotic stimuli initiate *MLL-AF9* translocations that are transcribed in cells capable of division. Cancer Res 63:1377–1381
17. Pfeifer GP, Riggs AD (1996) Genomic sequencing by ligation-mediated PCR. Mol Biotechnol 5:281–288
18. Drouin R, Therrien J-P, Angers M, Ouellet S (2001) In vivo DNA analysis. In: Moss T (ed) DNA-protein interactions—principles and protocols. Methods in molecular biology, vol 148. Humana Press, Totowa, NJ, pp 175–219
19. Grimaldi KA, McAdam SR, Souhami RL, Hartley JA (1994) DNA damage by anti-cancer agents resolved at the nucleotide level of a single copy gene: evidence for a novel binding site for cisplatin in cells. Nucleic Acids Res 22:2311–2317
20. Komura J, Riggs AD (1998) Terminal transferase-dependent PCR: a versatile and sensitive method for in vivo footprinting and detection of DNA adducts. Nucleic Acids Res 26:1807–1811
21. Danks MK, Schmidt CA, Cirtain MC, Suttle DP, Beck WT (1988) Altered catalytic activity of and DNA cleavage by DNA topoisomerase II from human leukemic cells selected for resistance to VM-26. Biochemistry 27:8861–8869
22. Bugg BY, Danks MK, Beck WT, Suttle DP (1991) Expression of a mutant DNA topoisomerase II in CCRF-CEM human leukemic cells selected for resistance to teniposide. Proc Natl Acad Sci USA 88:7654–7658
23. Bromberg KD, Osheroff N (2001) DNA cleavage and religation by human topoisomerase IIα at high temperature. Biochemistry 40:8410–8418
24. Angers M, Cloutier JF, Castonguay A, Drouin R (2001) Optimal conditions to use *Pfu* exo$^-$ DNA polymerase for highly efficient ligation-mediated polymerase chain reaction protocols. Nucleic Acids Res 29:E83
25. Gu Y, Alder H, Nakamura T, Schichman SA, Prasad R, Canaani O, Saito H, Croce CM, Canaani E (1994) Sequence analysis of the breakpoint cluster region in the ALL-1 gene involved in acute leukemia. Cancer Res 54:2326–2330
26. Patenaude A, Ven Murthy MR, Mirault ME (2004) Mitochondrial thioredoxin system: effects of TrxR2 overexpression on redox balance, cell growth, and apoptosis. J Biol Chem 279: 27302–27314
27. Joel SP, Shah R, Clark PI, Slevin ML (1996) Predicting etoposide toxicity: relationship to organ function and protein binding. J Clin Oncol 14:257–267
28. Sordet O, Khan QA, Plo I, Pourquier P, Urasaki Y, Yoshida A, Antony S, Kohlhagen G, Solary E, Saparbaev M, Laval J, Pommier Y (2004) Apoptotic topoisomerase I-DNA complexes induced by staurosporine-mediated oxygen radicals. J Biol Chem 279:50499–50504
29. Sordet O, Liao Z, Liu H, Antony S, Stevens EV, Kohlhagen G, Fu H, Pommier Y (2004) Topoisomerase I-DNA complexes contribute to arsenic trioxide-induced apoptosis. J Biol Chem 279:33968–33975
30. Raffini LJ, Slater DJ, Rappaport EF, Lo Nigro L, Cheung NK, Biegel JA, Nowell PC, Lange BJ, Felix CA (2002) Panhandle and reverse-panhandle PCR enable cloning of der(11) and der(other) genomic breakpoint junctions of *MLL* translocations and identify complex translocation of *MLL, AF-4,* and *CDK6*. Proc Natl Acad Sci USA 99:4568–4573
31. Langer T, Metzler M, Reinhardt D, Viehmann S, Borkhardt A, Reichel M, Stanulla M, Schrappe M, Creutzig U, Ritter J, Leis T, Jacobs U, Harbott J, Beck JD, Rascher W, Repp R (2003) Analysis of t(9;11) chromosomal breakpoint sequences in childhood acute leukemia: almost identical *MLL* breakpoints in therapy-related AML after treatment without etoposides. Genes Chromosomes Cancer 36:393–401
32. Zhang Y, Zeleznik-Le N, Emmanuel N, Jayathilaka N, Chen J, Strissel P, Strick R, Li L, Neilly MB, Taki T, Hayashi Y, Kaneko Y, Schlegelberger B, Rowley JD (2004) Characterization of genomic breakpoints in *MLL* and *CBP* in leukemia patients with t(11;16). Genes Chromosomes Cancer 41:257–265
33. Gillert E, Leis T, Repp R, Reichel M, Hosch A, Breitenlohner I, Angermuller S, Borkhardt A, Harbott J, Lampert F, Griesinger F, Greil J, Fey GH, Marschalek R (1999) A DNA damage repair mechanism is involved in the origin of chromosomal translocations t(4;11) in primary leukemic cells. Oncogene 18:4663–4671

34. Reichel M, Gillert E, Angermuller S, Hensel JP, Heidel F, Lode M, Leis T, Biondi A, Haas OA, Strehl S, Panzer-Grumayer ER, Griesinger F, Beck JD, Greil J, Fey GH, Uckun FM, Marschalek R (2001) Biased distribution of chromosomal breakpoints involving the *MLL* gene in infants versus children and adults with t(4;11) ALL. Oncogene 20:2900–2907
35. Betti CJ, Villalobos MJ, Diaz MO, Vaughan AT (2001) Apoptotic triggers initiate translocations within the *MLL* gene involving the nonhomologous end joining repair system. Cancer Res 61:4550–4555
36. Durrieu F, Samejima K, Fortune JM, Kandels-Lewis S, Osheroff N, Earnshaw WC (2000) DNA topoisomerase IIα interacts with CAD nuclease and is involved in chromatin condensation during apoptotic execution. Curr Biol 10:923–926
37. Meyer C, Schneider B, Reichel M, Angermueller S, Strehl S, Schnittger S, Schoch C, Jansen MW, van Dongen JJ, Pieters R, Haas OA, Dingermann T, Klingebiel T, Marschalek R (2005) Diagnostic tool for the identification of *MLL* rearrangements including unknown partner genes. Proc Natl Acad Sci USA 102:449–454
38. Aplan PD, Chervinsky DS, Stanulla M, Burhans WC (1996) Site-specific DNA cleavage within the *MLL* breakpoint cluster region induced by topoisomerase II inhibitors. Blood 87: 2649–2658
39. Broeker PL, Super HG, Thirman MJ, Pomykala H, Yonebayashi Y, Tanabe S, Zeleznik Le N, Rowley JD (1996) Distribution of 11q23 breakpoints within the *MLL* breakpoint cluster region in de novo acute leukemia and in treatment-related acute myeloid leukemia: correlation with scaffold attachment regions and topoisomerase II consensus binding sites. Blood 87:1912–1922
40. Long BH, Musial ST, Brattain MG (1985) Single- and double-strand DNA breakage and repair in human lung adenocarcinoma cells exposed to etoposide and teniposide. Cancer Res 45:3106–3112
41. Osheroff N (1989) Effect of antineoplastic agents on the DNA cleavage/religation reaction of eukaryotic topoisomerase II: inhibition of DNA religation by etoposide. Biochemistry 28: 6157–6160
42. Bromberg KD, Burgin AB, Osheroff N (2003) A two-drug model for etoposide action against human topoisomerase IIα. J Biol Chem 278:7406–7412
43. Hsiang YH, Lihou MG, Liu LF (1989) Arrest of replication forks by drug-stabilized topoisomerase I-DNA cleavable complexes as a mechanism of cell killing by camptothecin. Cancer Res 49:5077–5082
44. Furuta T, Takemura H, Liao ZY, Aune GJ, Redon C, Sedelnikova OA, Pilch DR, Rogakou EP, Celeste A, Chen HT, Nussenzweig A, Aladjem MI, Bonner WM, Pommier Y (2003) Phosphorylation of histone H2AX and activation of Mre11, Rad50, and Nbs1 in response to replication-dependent DNA double-strand breaks induced by mammalian DNA topoisomerase I cleavage complexes. J Biol Chem 278:20303–20312
45. Strissel PL, Strick R, Rowley JD, Zeleznik-Le NJ (1998) An in vivo topoisomerase II cleavage site and a DNase I hypersensitive site colocalize near exon 9 in the *MLL* breakpoint cluster region. Blood 92:3793–3803
46. Strissel PL, Strick R, Tomek RJ, Roe BA, Rowley JD, Zeleznik-Le NJ (2000) DNA structural properties of *AF9* are similar to *MLL* and could act as recombination hot spots resulting in *MLL/AF9* translocations and leukemogenesis. Hum Mol Genet 9:1671–1679
47. Nilson I, Lochner K, Siegler G, Greil J, Beck JD, Fey GH, Marschalek R (1996) Exon/intron structure of the human ALL-1 (MLL) gene involved in translocations to chromosomal region 11q23 and acute leukaemias. Br J Haematol 93:966–972
48. Vaughan AT, Betti CJ, Villalobos MJ (2002) Surviving apoptosis. Apoptosis 7:173–177
49. Rowley JD (2001) Chromosome translocations: dangerous liaisons revisited. Nat Rev Cancer 1:245–250
50. Sordet O, Khan QA, Kohn KW, Pommier Y (2003) Apoptosis induced by topoisomerase inhibitors. Curr Med Chem Anticancer Agents 3:271–290
51. Pourquier P, Pilon AA, Kohlhagen G, Mazumder A, Sharma A, Pommier Y (1997) Trapping of mammalian topoisomerase I and recombinations induced by damaged DNA containing nicks or gaps: importance of DNA end phosphorylation and camptothecin effects. J Biol Chem 272:26441–26447
52. Borgnetto ME, Tinelli S, Carminati L, Capranico G (1999) Genomic sites of topoisomerase II activity determined by comparing DNA breakage enhanced by three distinct poisons. J Mol Biol 285:545–554
53. Keeney S, Giroux CN, Kleckner N (1997) Meiosis-specific DNA double-strand breaks are catalyzed by Spo11, a member of a widely conserved protein family. Cell 88:375–384